# PROTOTYPE DEVELOPMENT FOR VEHICLE BASED LASER MAPPING SYSTEM (VLMS)

**Dinesh MANANDHAR, Ryosuke SHIBASAKI**
**The University of Tokyo, Japan**
**Centre for Spatial Information Science and**
**Institute of Industrial Science**
**4-6-1, Komaba, Meguro-ku, Tokyo 153-8505, JAPAN**
dinesh@skl.iis.u-tokyo.ac.jp, shiba@skl.iis.u-tokyo.ac.jp

**KEY WORDS:** Mobile Mapping, Calibration, Range Data, CCD Image, GPS/INS

## ABSTRACT

In this research, a prototype for Vehicle based Laser Mapping System (VLMS) is developed, which is used for the development of 3-D spatial database of urban objects. In the prototype, we use laser scanner as the main sensor for data acquisition and omni-direction CCD camera for supplementing further information as necessary. Since, the laser scanner and the omni-direction camera observe the same object simultaneously, the textual data from the CCD camera can be directly overlaid on to the three dimension coordinate data from the laser scanner. This aids in solving the region of uncertainties or conflicts. Four sets of such sensor systems are used. The use of four sets of omni-direction camera assist us in extracting the "hidden" features (e.g. buildings blocked by trees or moving vehicles) as well as provides us multiple choice of images taken from different view point. The use of omni-direction camera for mobile mapping system is rather new. The navigation component, as usual, consists of GPS and INS for geo-referencing purpose.

The main discussion in this paper is about the system configuration, calibration of sensors (CCD camera and Laser scanner), analysis of Hybrid Inertial Survey System (HISS) data and laser range data. HISS is the combination of either GPS and INS or Odometer and INS. The discussion includes a brief introduction of algorithms used and calibration procedural. Algorithms are developed to solve the unknown intrinsic and extrinsic parameters both for the CCD camera and laser scanner. We have also listed some of the practical difficulties with such type of mobile mapping system.

## 1 INTRODUCTION

The present contest of rapid growth and development of urban area demands regular acquisition and/or updating of spatial data preferably in three dimensions for effective and efficient planning and management. The vehicle-based mapping system has an immense value in present days for fulfilling the demands of fast and cost-effective data acquisition for GIS and other mapping related fields. It has flexibility in providing multi temporal, multi dimensional and multi resolution data. This led us towards the development of the vehicle-based laser mapping system. In most of such systems only CCD or Video camera are used for image data and GPS/INS are used for positioning. However, in our case we are using laser scanner that provides a cloud of range points in three dimensions. Use of laser scanners for mobile mapping is rather new concept.

The vehicle-based laser mapping system comprises of three basic components, viz. Laser Scanner, CCD camera and GPS/INS. The main unit for data acquisition is Laser Scanner, which provides range data (angle and distance from the sensor to each of the observed feature). These data can easily be converted into 3-dimensional coordinates of the scanned features with respect to the sensor position or to the real world origin. In the later case, the real world coordinate reference is provided by using either the combination of GPS and INS or Odometer and INS. However the information, we get from the laser scanner are just a set of bare 3-dimensional coordinates. It has no information about the texture or color of the features scanned. In order to fulfill, this deficiency, we use CCD cameras. Since, the laser scanner and the CCD camera observe the same object simultaneously, the textual data from the CCD camera can be directly overlaid to the three dimension coordinate data from the laser scanner. We have used four sets of sensors (Laser and CCD) fixed on top of the vehicle at different angles. This configuration provides us more visibility to capture the features even if it is occluded in one of the sensors. Using this system (vehicle based laser), we can build the urban 3-D database at much higher resolution and accuracy. This type of system is unique on it-self as ground based laser scanners have not be used for data acquisition for developing urban 3-D maps, although there are quite a lot of applications and research on airborne laser scanning system.

## 2 SYSTEM CONFIGURATION

The mobile mapping vehicle is shown in figure 1. It consists of four CCD cameras, four laser scanners, Hybrid Inertial Survey System (HISS) which consists of DGPS, INS and electronic Odometer for position and orientation data.

Figure 1. Mobile Mapping Survey Vehicle and the Sensors on top of the vehicle

### 2.1 HISS (The GPS/INS Integration)

The Hybrid Inertial Survey System (HISS) is the integration of GPS and INS. GPS can provide 3-dimension positioning as far as at least four GPS satellites are visible. The GPS is operated in differential mode, which can provide positional accuracy (standard deviation) of about one meter with a PDOP better than 3, while in static mode after initialization. However, when the GPS antenna is obstructed by trees or buildings, the accuracy is either seriously degraded or the positioning data is not available at all due to lesser number of visible satellites or higher PDOP value. The INS can measure position autonomously with high precision but it is highly affected by drift error. Thus the combination of both the GPS and INS results in better positioning data. However, the problem still exists, if the GPS data is not available for longer time period, which is quite possible in field surveying in urban area. In order to avoid this problem an electronic wheel odometer is also integrated with the GPS/INS system. The odometer data is automatically used once the GPS positioning is not satisfactory. The decision is based on these two factors: when the number of satellites are less than four or when the PDOP is greater than four. Kalman filter is used for integrating the systems. The HISS output is based on either GPS/INS mode or Odometer/INS mode. For details on HISS and it's field test results, refer Tamura (1998).

### 2.2 Laser Scanner

Four laser scanners are fixed on top of the vehicle at four different directions as shown in figure 1. The purpose of using four units is to capture the data from different viewing angle so that as much of data can be extracted as possible even when the target is occluded by pedestrians or moving vehicles. The configuration of laser scanner is given in Table 1.

| | |
|---|---|
| Meas. Distance Range | 50m(reflection rate 20%) |
| Accuracy of Range | 3cm(1 $\sigma$) |
| Scanning Rotation | 300° |
| Angular Range Step | 0.25° |
| Frequency | 10Hz |

Table 1. Laser Scanner configuration

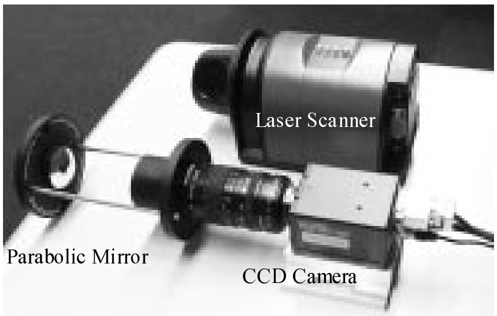


Figure 2. CCD and Laser sensor units

### 2.3 CCD Camera

Four CCD cameras are used with parabolic reflecting mirrors. Each unit of CCD camera and Laser scanner are housed in a single frame. Table 2 shows the configuration of the CCD camera.

| | |
|---|---|
| Photography Element | 1/2 inch color CCD |
| Resolution | 659x494 |
| ESD Output | RGB |
| Trigger shutter | 1/60～1/10000 |
| Lens Mount | C mount |

Table 2. Configuration of CCD Camera

## 3 DEVELOPMENT PROCESS

### 3.1 Calibration

The foremost task is to calibrate each individual sensor. In this regard, we have developed the algorithms and conducted experiments for calibration of Laser Scanners and CCD cameras. The experiments were conducted both indoors and outdoors. The indoor experiments are necessary to calibrate the laser scanner and CCD camera using parabolic mirrors.

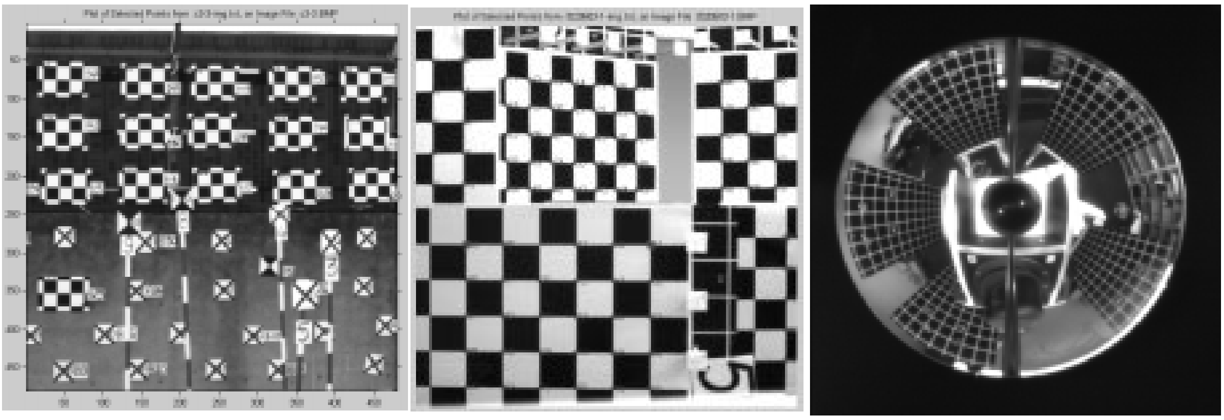

Figure 3. Type of targets used for outdoors, indoors and omni CCD calibration

### 3.2 CCD Calibration

The calibration of CCD camera is conducted to find out the intrinsic (focal length, principal point and lens distortions) and extrinsic (position and attitude of the camera) parameters. The extrinsic parameters are necessary to integrate with laser scanner as well as with other sensor units and ultimately to transfer to the local map coordinate system. The algorithm, we have used is based on DLT (Direct Linear Transform), Abdel-Aziz (1971). The details are not given here as many researchers have already published on it. For details, please, refer Abdel-Aziz (1971). In our case, we solved the calibration problem in two steps. In the first step, DLT is used from which eleven L-parameters are computed. These L-parameters are used as initial estimate values of the parameters for the non-linear computation. There are different methods to extract the camera intrinsic and extrinsic parameters from the 11-Lparameters. The one, we have used is briefly mentioned here. The detail derivation of the algorithm will be available through our web site (http://shiba.iis.u-tokyo.ac.jp) in near future.

3.2.1 **DLT Algorithm.** The DLT method is based on pinhole camera model and does not consider the lens distortions like radial and tangential distortions. The DLT equations are :

$$u = \frac{L_1 X + L_2 Y + L_3 Z + L_4}{L_9 X + L_{10} Y + L_{11} + Z + 1} \tag{1}$$

$$v = \frac{L_5 X + L_6 Y + L_7 Z + L_8}{L_9 X + L_{10} Y + L_{11} + Z + 1} \tag{2}$$

where, u, v are image coordinates in camera coordinate system, and X,Y,Z are object coordinates in local coordinate system, $L_1 \ldots\ldots L_{11}$ are eleven DLT parameters. We have built the constraint by assigning value one to $L_{12}$ parameter. In this case the linear equation can be solved with pseudo inverse. Faugeras and Toscani (1987), suggested the constraint $L^2_9 + L^2_{10} + L^2_{11} = 1$, which is singularity free. The following equations explain the computation of L-parameters and extraction of camera intrinsic and extrinsic parameters from these L-parameters.

The equations 1 and 2 above can be written in matrix form as

$$\begin{bmatrix} X & Y & Z & 1 & 0 & 0 & 0 & 0 & -uX & -uY & -uZ \\ 0 & 0 & 0 & 0 & X & Y & Z & 1 & -vX & -vY & -vZ \end{bmatrix} * \begin{bmatrix} L_1 \\ : \\ : \\ L_{11} \end{bmatrix} = \begin{bmatrix} u \\ v \end{bmatrix} \tag{3}$$

Equation 3 can be solved directly as a*L=b in least square fashion. The solution is given by

$$L = pinv(a^t * a) * (a^t * b) \tag{4}$$

There are different ways to extract the camera intrinsic and extrinsic parameters from the eleven L-parameters. For details, refer Melen (1994), or Kwon (1999). Melen used the RQ decomposition method. However, the computed results from DLT are not satisfactorily enough, as we can not incorporate the lens distortions. Their exists different version of DLT which also incorporates the lens distortion parameters. Hatze (1988) has proposed Modified DLT (MDLT) method which considers the lens distortions as well.

In the second step, the calibration is performed considering the lens distortion parameters as well. This is accomplished by minimizing the residual between the actual observation values of image coordinates (U,V) and the computed values of (u,v) by using the computed camera parameters. The objective is to minimize the sum of square of residuals:

$$\sum_{i=1}^{n}(U_i - u_i)^2 + \sum_{i=1}^{n}(V_i - v_i)^2 \Rightarrow \min \tag{5}$$

Non-linear least square estimation technique can be used to solve equation 5. We have used the Lavenberg-Marquardt algorithm for the non-linear optimization. The proper initial values are obtained from the DLT method. Without proper initial value the solution might stick to local minimum. The Matlab functions written by Hekkilla and Silven have been used for solving the non-linear least square function.

### 3.3 Laser Calibration

The laser scanner calibration was conducted indoors. The calibration of laser scanner outdoors is difficult due to the difficulty in identifying the reflected pulses from the feature on the data. A special arrangement for the laser targets was made for easy identification of reflected pulses. During the calibration experiments, we have also conducted for the accuracy check of the range data.

**3.3.1 Laser Calibration Algorithm.** The laser calibration algorithm is given below. This is a seven-parameter transformation for transformation of coordinates from one system to another system. Using this algorithm, we simply get the exterior orientation of the laser scanner, which is needed for integrated calibration with CCD camera and/or other sensors. The algorithm is:

$$\begin{bmatrix} x \\ y \\ z \end{bmatrix} = s \begin{bmatrix} r_1 & r_2 & r_3 \\ r_4 & r_5 & r_6 \\ r_7 & r_8 & r_9 \end{bmatrix} \begin{bmatrix} X \\ Y \\ Z \end{bmatrix} + \begin{bmatrix} T_1 \\ T_2 \\ T_3 \end{bmatrix} \tag{6}$$

Equation 6 can be expressed as $x = sRX + T$ or in functional form $f = sRX + T - x = 0$ (7)

where, x is the target coordinates in laser coordinate system, X is the target coordinates in the local coordinate system (in this case total station survey coordinates), s is the scale factor, R is the rotation matrix and T is the translation vector.

Considering both x and X as observations, equation 7 can be linearized as $Av + B\Delta = f$ where (8)

$$A = \lfloor s^0 M^0 \quad -I_{3x3} \rfloor \qquad v = \begin{bmatrix} v_x \\ v_X \end{bmatrix} \qquad B = \lfloor M^0 X \quad s^0 M_1^0 X \quad s^0 M_2^0 X \quad s^0 M_3^0 X \quad I_{3x3} \rfloor \tag{9}$$

$M_1$, $M_2$, $M_3$ are partial derivatives of M with respect to $\omega$, $\varphi$, and $\kappa$ respectively

$$\Delta = \lfloor \delta s \quad \delta_1 \quad \delta_2 \quad \delta_3 \quad \delta T_1 \quad \delta T_2 \quad \delta T_3 \rfloor^t \tag{10}$$

If we assume that all the observations have equal weight and are uncorrelated, then we can solve equation 8 as

$$\Delta = pinv(B^t * B) * (B^t * f) \tag{11}$$

$\Delta$ is the estimated value to be added to the initial approximation. Since, the equation is non-linear, iteration must be done to achieve the most probable estimation for all the unknown parameters, like scale, three rotation angles and the translation vector.

### 3.4 GPS/INS

The integrated DGPS/INS system, which is called HISS, was developed by Asia Air Survey. The integrated system has an accuracy of about one-meter in horizontal plane. The system once initialized can work either on DGPS/INS mode or Odometer/INS mode. The switching between the two modes is automatic, which is based on the PDOP (if PDOP > 4.0) and number of visible satellites (if no. of sat < 4). The preference is always given to DGPS/INS mode. We have conducted some tests to see the behavior of the DGPS alone and DGPS/INS results at stationary mode (while the vehicle is not moving).

### 3.5 Data Acquisition Mechanism

Data is acquired after every specific distance. In this case, data is acquired every 20cm. Once the vehicle has traveled forward by a specified distance, trigger is activated which time tags the HISS data and captures the CCD image frame and Laser scanner data. The trigger setting can be controlled by the user depending upon the requirement. Data is temporarily stored in the memory. The PC has 512MB of memory, which limits the continuos operation of the data acquisition. Data has to be saved into the hard disk after every 40-50m.

## 4 RESULTS AND DISCUSSIONS

The results of CCD camera calibration, Laser Sensor calibration and HISS output are presented below.

### 4.1 CCD Camera Calibration

The results presented here for the CCD camera are without using the parabolic reflecting mirror. The use of parabolic mirror drastically reduces the image resolution. Thus, we would like to calibrate the CCD camera both with and without the mirror. We expect that the results without using the mirror are better than the one using the mirror. These calibration results will be used for integrated calibration with GPS/INS. The integrated calibration with laser should be done using the parabolic mirror, as the laser data have to be overlaid on the CCD image.

| Camera | Scale | Focal (mm) | U0 (pix) | V0 (pix) | rad1 | rad2 | tan1 | tan2 | Error (pix) |
|---|---|---|---|---|---|---|---|---|---|
| C1 | 1.034 | 12.20 | 224.16 | 222.03 | 8.94E-04 | -2.07E-04 | -6.85E-04 | -3.06E-04 | 0.64 |
| C2 | 1.034 | 12.48 | 237.78 | 248.76 | 4.73E-04 | -9.59E-05 | -2.00E-04 | -3.47E-05 | 0.77 |
| C3 | 1.034 | 12.30 | 251.95 | 262.72 | 2.21E-03 | -3.07E-04 | 4.43E-05 | 1.70E-04 | 0.56 |

| Camera | X0(mm) | Y0(mm) | Z0(mm) | Omg (deg) | Phi (deg) | Kappa (deg) |
|---|---|---|---|---|---|---|
| C1 | -3880 | -2714 | 2552 | 90.88 | -0.87 | 179.73 |
| C2 | -3671 | -3229 | 2624 | 90.41 | -0.96 | -179.85 |
| C3 | -4043 | -1824 | 2680 | 89.96 | 5.62 | -179.57 |

Table 3. CCD camera calibration parameters for outdoor experiment

| Camera | Scale | Focal | U0 | V0 | Rad1 | Rad2 | Tang1 | Tang2 | Error |
|---|---|---|---|---|---|---|---|---|---|
| C3 | 1.029 | 12.363 | 234.73 | 293.02 | 1.71E-03 | -2.88E-04 | -2.94E-04 | 1.26E-04 | 0.76 |
| C4 | 1.027 | 12.783 | 243.58 | 214.86 | -8.93E-04 | -3.50E-05 | -3.45E-04 | -6.99E-06 | 0.70 |
| C1 | 1.029 | 12.825 | 227.07 | 217.37 | -1.07E-03 | -5.16E-07 | -2.60E-04 | -9.67E-05 | 0.65 |
| C2 | 1.028 | 12.723 | 254.73 | 226.98 | -6.42E-04 | -5.77E-05 | -1.74E-04 | 2.70E-04 | 0.70 |

| Camera | X0(mm) | Y0(mm) | Z0(mm) | Omg | Phi | Kappa |
|---|---|---|---|---|---|---|
| C3 | -1125 | -2872 | 918 | 87.09 | 34.81 | 178.84 |
| C4 | -1140 | -2830 | 740 | 91.41 | 35.15 | 181.26 |
| C1 | -1111 | -2508 | 747 | 91.17 | 34.02 | 180.73 |
| C2 | -1057 | -2836 | 1076 | 86.32 | 34.08 | 178.33 |

Table 4. CCD camera calibration parameters for indoor experiment

Although, the calibration results shown above list the overall error (sum of square of errors) better than one pixel, the error (standard deviation) in estimating the individual intrinsic parameters varied a lot from each of the calibration. The variation was 2-8 pixels. This may be due to the errors introduced in extracting the target image coordinates as well as measuring the targets in real world coordinates (target survey error). We have used the targets as shown in figure 3 for outdoors, indoors and omni CCD calibration. We feel that the design and type of target affects the simplicity and accuracy of the coordinate extraction. The targets must be designed based on calibration and surrounding environment.

In the next experiment, we will also use circular targets to see how the results are affected. The target point, which is the circle centre will be automatically extracted based on the ellipse model and extracting the boundary of the circle, rather than the edge of the circle (edge extraction).

### 4.2 Laser Scanner Calibration

The laser calibration results for the extrinsic parameters are given in Table 5. The difficult part in laser calibration is to identify the reflected target points on the cloud of the laser target data. We fixed the targets of size four sq.cm. (target used for total station survey) on the tips of wooded rods which are fixed on a board, projected toward the sensor direction. This gives a cloud of points at the same plane plus a few reflected target points at nearer distance from other cloud of points. This simplifies the identification of the target-reflected points. Besides, extrinsic parameter estimation, the precision of the scanner itself is carried out. This is achieved by measuring the height of the wall by the scanner and the total station, see figure 4. Table 6 shows the results. The discrepancy is about 3-5 cm.

| Xo (mtr) | Yo (mtr) | Zo (mtr) | Omega | Phi | Kappa |
|---|---|---|---|---|---|
| 3.236 | 1.625 | 0.630 | 17.4 | 2.8 | 178.28 |

Table 5. Laser Sensor extrinsic calibration parameters

| | Sensor1 | Sensor2 | Sensor3 | Sensor4 |
|---|---|---|---|---|
| Position1 | 2.668 | 2.685 | 2.697 | 2.694 |
| Position2 | 2.694 | 2.670 | 2.691 | 2.692 |
| Position3 | 2.685 | 2.707 | 2.709 | 2.704 |

Table 6. Height measurement by Laser scanner. The actual wall height is 2.70mtr.

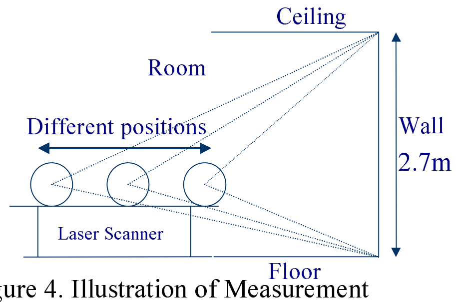


Figure 4. Illustration of Measurement of Wall by Laser Scanner

Figure 5, shows the laser range image acquired by one of the sensors. The image is from uncalibrated range data. The vehicle speed during the acquisition of this data is around 5-10km/hr, which is too slow for practical implementation. The building face is tilted which is due to the use of uncalibrated data. The HISS data are directly assigned to the laser range points. This is just to see how the laser range data (and different features, like buildings, roads, trees) look like when acquired from a moving platform. We can see some trees at the left side of the image and at the centre of the road, neatly trimmed plants in the traffic island are seen.

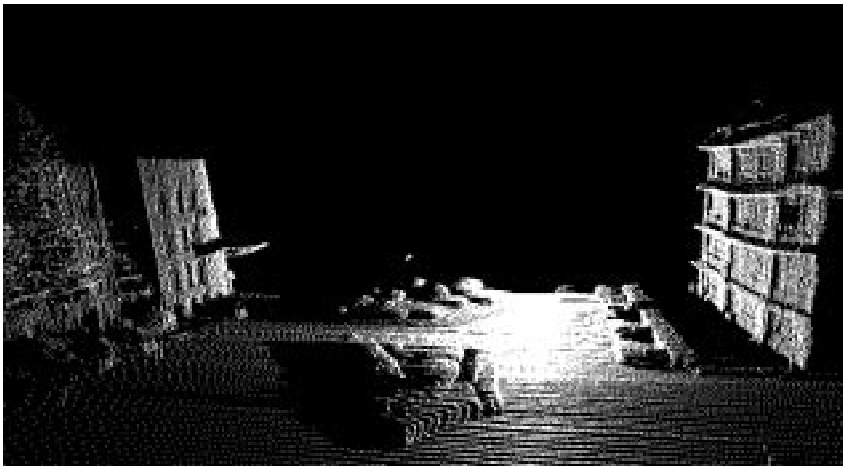

Figure 5. Laser Range Image

### 4.3 HISS Observation

Figure 6 shows the height data observed in static mode. The observation was done for about 15 minutes, after initializing the HISS system, which normally takes 15~20 minutes. We can see how the DGPS data and DGPS/INS data behaves. The height data has become constant, once the HISS mode has switched to Odometer/INS mode. The value is constant because there was no input (or only constant input) from the Odometer as the vehicle was in static mode. The HISS output for mean and standard deviation of the height is 69.122m and 0.9165m respectively. Figure 7, shows the HISS position (horizontal) output. The graph is plotted for position data for three-consecutive vehicle drives. The vehicle was stopped intermittently between the observations for data transfer from the memory to hard disk. The HISS output is based on Kalman filtering of either DGPS / INS or Odometer / INS data. However, initialization is always accomplished with DGPS/INS mode for at least 15 minutes. It was observed that the transition from DGPS/INS mode to Odometer/INS mode was smooth. However, we can also notice the sudden jump of position data when the HISS output changed from Odometer/INS mode to DGPS/INS mode. It happened when the vehicle was stopped for some time (2-3min) and then moved again.

### 4.4 Practical Difficulties

At present, the vehicle should be driven slowly (~10km/hr) and stopped after certain distance traveled (~45mtr). This is quite slow and unpractical to survey in urban area. The limitation is due to the scanning frequency (10Hz) of the Laser Scanner and PC hardware. In order to acquire the data at faster rate the laser scanning frequency should be higher than 10Hz. The PC has 512MB memory, which limits the continuous observation. After every, 40-50m observation, the data has to be transferred from the memory to the hard disk. Data is captured at every 20cm of distance traveled. It is difficult to identify the laser target points reflected by the targets.

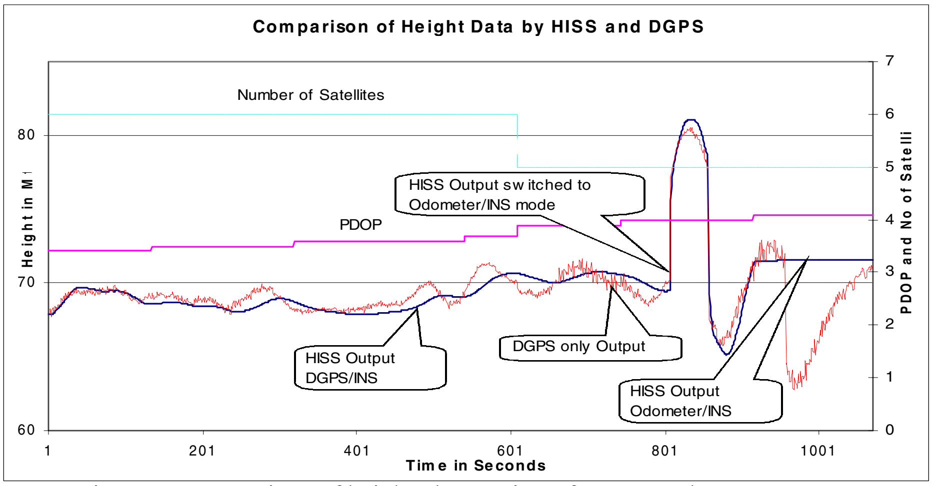


Figure 6. Comparison of height observation of DGPS and HISS output

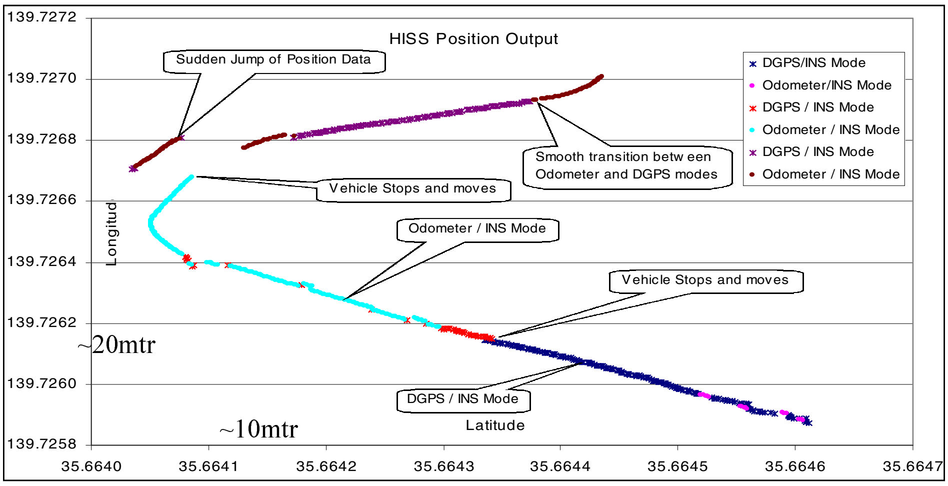


Figure 7. HISS position output under different modes

## 5 CONCLUSION AND FUTURE WORKS

The individual calibration of CCD camera and laser scanner has been completed. Some preliminary data has been acquired by using the system. The laser range data is promising for developing 3-D urban GIS database. HISS output has been analyzed and needs further improvement to handle the situation when the position data suddenly jumps from it's true position. The results show that, it still needs improvement in CCD calibration in order to make the computation more robust. The target coordinate extraction errors should be minimized and accounted in computation. This is an ongoing research with main objective of feature extraction from range data for building three dimensions urban GIS database. The future work mainly consists of two parts; the first one is CCD omni camera calibration and integrated calibration of all the sensors. The second part is feature extraction and classification of range image data. We will limit the objectives primarily to the extraction of buildings or building faces, roads and trees. These features will be extracted by filtering the pedestrians and the moving vehicles as far as possible.


## ACKNOWLEDGEMENTS

The authors would like to acknowledge Asia Air Survey, Japan for their assistance in conducting the calibration field tests. Equally, we would also like to acknowledge the help of Tianen Chen, Hujin Zhao and Kazuhisa Inaba.

## REFERENCES

Abdel-Aziz, Y.I. and Karara, H.M., 1971, Direct linear transformation into object space coordinates in close-range photogrammetry, Proc. Symposium on Close Range Photogrammetry, Urbana, Illinois, p. 1-18

Brown, D.C., 1971, Close Range Camera Calibration, Photogrammetric Engineering, vol 37, no 8

Faig, W., 1975, Calibration of close-range photogrammetric systems: Mathematical formulation. Photogrammetric Engineering and Remote Sensing , vol. 41, no 12, p. 1479-1486

Faugeras, O.D and Toscani, G. ,1987, Camera calibration for 3D computer vision, Proc. Of International workshop on Industrial Applications for Machine Vision and Machine Intelligence, Silken, Japan, p. 240-247

Fraser, C.S., 1997, Digital camera self calibration, ISPRS Journal of Photogrammetry and remote sensing, vol 52, p149-159

Hatze, H., 1988, High Precision three dimensional photogrammetric calibration and object space reconstruction using a modifiied DLT approach, Journal of Biomechanics, Vol 21, p. 533-538.

Heikkila, J., and Silven, O., A four step camera calibration procedure with implicit image correction, Department of Electrical Engineering, University of Oulu, jth@ee.oulu.fi

Kwon, Y., http://www.cs.bsu.edu/~ykwon

Melen T., 1994, Geometrical modelling and calibration of video cameras for underwater navigation, Dr. Ing. Thesis, Norges Tekniske Hogskole, Institute for Teknisk Kybernetikk

Mikhail, E. M., Observations and Least Squares, Harper and Row publishers, ISBN 0-7002-24811-5

Tamura, T., Kitagawa, T., Tsuji, K., Uchida O., Shimogaki, Y., The GPS/INS integration and kinematic photogrammetry for mobile mapping system, International Archives of Photogrammetry and Remote Sensing, vol. XXXII, part 5, pp. 824-829, Hakodate 1998.

Tsai, R.Y., 1987, A versatile camera calibration technique for high accuracy 3D machine vision metrology using off the shelf TV cameras and lenses, IEEE Journal of Robotics and Automation, vol. RA3, p. 323--344, August 1987